Available online at www.sciencedirect.com
ScienceDirect
Journal of Organometallic Chemistry 692 (2007) 175–183
Journal of Organometallic Chemistry
www.elsevier.com/locate/jorganchem

Dinuclear Rh(I) complex with 2,7-bis(diphenylphosphino)-1,8-naphthyridine: Synthesis, structure, and dynamic property

Tomoaki Tanase *, Hiroe Takenaka, Eri Goto

Department of Chemistry, Faculty of Science, Nara Women's University, Kitauoya-higashi-machi, Nara, 630-8285, Japan

Received 10 March 2006; received in revised form 12 May 2006; accepted 16 May 2006
Available online 8 September 2006

Abstract

Reaction of $[RhCl(cod)]_2$ with 2,7-bis(diphenylphosphino)-1,8-naphthyridine (dpnapy) and 2,6-xylyl isocyanide (XylNC) in the presence of NH_4PF_6 afforded the dirhodium(I) complex, $[Rh_2(\mu\text{-dpnapy})_2(XylNC)_4](PF_6)_2$ (**5**), and similar procedures using $[MCl_2(cod)]$ (M = Pt, Pd) resulted in the formation of $[Pt_2(\mu\text{-dpnapy})_2(XylNC)_4](PF_6)_4$ (**6**) and $[Pd_2Cl_2(\mu\text{-dpnapy})_2(XylNC)_2](PF_6)_2$ (**7**). Complexes **5**–**7** were characterized by elemental analysis, IR, UV–Vis, ^1H and $^{31}P\{^1H\}$ NMR, and ESI mass spectroscopic techniques, to involve a small and rigid d^8 $\{M_2(\mu\text{-dpnapy})_2\}$ metallomacrocycle. Complex **5** readily incorporated a silver(I) ion into the macrocycle to afford $[Rh_2Ag(\mu\text{-dpnapy})_2(XylNC)_4](PF_6)_3$ (**8**) which was characterized by X-ray crystallography. The Ag(I) ion is trapped by two *trans* N atoms of dpnapy ligands, resulting in an asymmetric Rh–Ag···Rh structure, determined as a disordered model in the crystal structure, and however, in a CH_2Cl_2 solution, a dynamic interconversion of the two Ag-trapped sites was observed with low-temperature NMR studies, which was further supported by DFT molecular orbital calculations. When an acetonitrile solution of complex **5** was treated over a droplet of mercury(0), the polymeric compound formulated as $\{[Rh(\mu\text{-dpnapy})(XylNC)_2](PF_6)\}_n$ (**9**) was isolated as yellow single crystals, which were revealed by X-ray crystallography to consist of C_6 helical rods along *c* axis with a pitch of 33.5 Å (rise of unit = 5.6 Å) and a diameter of 20.64 Å.

Keywords: Rhodium; Platinum; Dinuclear complexes; PNNP ligand; Metallomacrocycle; Helical polymer

1. Introduction

Multinuclear heterometallic complexes have attracted increasing attentions in developing multifunctional catalytic systems and electro- and photochemical materials [1]. The heterodonor ligands containing P and N atoms, such as 2,9-bis(diphenylphosphino)-1,10-phenanthroline (P_2phen) and 6,6′-bis(diphenylphosphino)-2,2′-bipyridine (P_2bpy), have been used to construct $\{M(\mu\text{-PNNP})_3M\}$ metallocryptands which encapsulate a heterometal atom in the large central cage; examples being $[M_2M'(\mu\text{-}P_2phen)_3]^{n+}$ (M = Au(I), Ag(I), Pt(0), Pd(0); M′ = Na(I), Tl(I), Pb(II), Hg(0), Hg_2^{2+}) [2–4]. In contrast, the linearly ordered PNNP ligand, 2,7-bis(diphenylphosphino)-1,8-naphthyridine (dpnapy), has potential to construct rigid and small cage with $\{M(\mu\text{-dpnapy})_3M\}$ framework and encapsulation of heteroatoms into the cage could afford linear multimetallic aggregations [5–9], and however, only few examples of multinuclear complexes with dpnapy ligands have been reported with $[Au_2M'(\mu\text{-dpnapy})_3]^{3+}$ (M′ = Na (**2a**) [7], K (**2b**) [6]), $[Ag_3(\mu\text{-dpnapy})_3]^{3+}$ (**2c**) [6,7], $[M_2Na(\mu\text{-dpnapy})_3L_2]^+$ (M = Pt, Pd; L = XylNC, CO (**3a**–**d**)) [8], and *trans*/*cis*-$[Mo_2(\mu\text{-}CH_3COO)_2(\mu\text{-dpnapy})_2]^{2+}$ (**4**) [9]. In complexes **2a** and **2b**, two trigonal Au(I) ions are coordinated by three phosphine groups of the dpnapy ligands and the sodium or potassium ion is tightly held at the center of D_3 symmetrical small cavity through six bonding interactions with the imine nitrogen

* Corresponding author. Fax: +81 742 20 3399.
E-mail address: tanase@cc.nara-wu.ac.jp (T. Tanase).

0022-328X/$ - see front matter © 2006 Elsevier B.V. All rights reserved.
doi:10.1016/j.jorganchem.2006.05.067

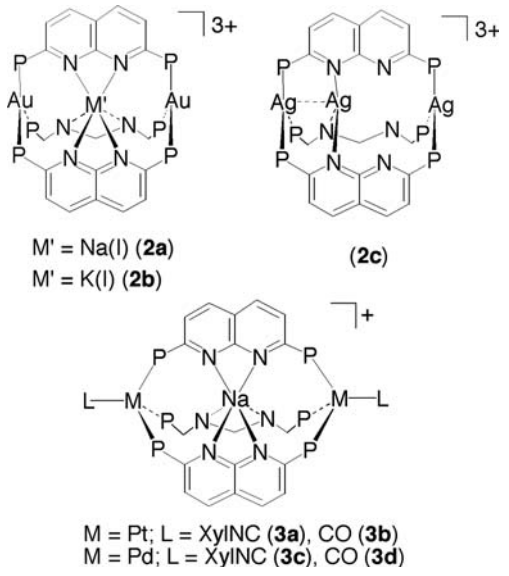

Scheme 1.

atoms (Scheme 1). Recently, we have reported the novel successive encapsulation of acidic hydrides into the rigid cavity of $[Pt_2Na(\mu\text{-dpnapy})_3(XylNC)_2]^+$ (**3a**), affording $[Pt_2Na(H)(\mu\text{-dpnapy})_3(XylNC)_2]^{2+}$ and $[Pt_2Na(H)_2(\mu\text{-dpnapy})_3(XylNC)_2]^{3+}$ in a stepwise fashion (Scheme 2) [8]. In contrast to the cage-type structures of $\{M(\mu\text{-dpnapy})_3M\}$ metallocryptands already reported, the metallomacrocycle of $\{M(\mu\text{-dpnapy})_2M\}$ was not prepared thus far, although it should be a more simple building block toward heterometallic systems.

In the present study, we have tried to synthesize the $\{M(\mu\text{-dpnapy})_2M\}$ metallomacrocycles by utilizing d^8 metal fragments and isolated dinuclear complexes of $[M_2(\mu\text{-dpnapy})_2(XylNC)_4](PF_6)_n$ (M = Rh, $n = 2$ (**5**); M = Pt, $n = 4$ (**6**)). Furthermore, complex **5** readily incorporated a silver(I) ion into the macrocycle to afford $[Rh_2Ag(\mu\text{-dpnapy})_2(XylNC)_2](PF_6)_3$ (**8**), which showed a dynamic site-exchange behavior of the trapped silver(I) ion, and complex **5** could also be transformed through metallocycle opening into the C_6 helical coordination polymer, $\{[Rh(\mu\text{-dpnapy})(XylNC)_2](PF_6)\}_n$ (**9**).

2. Experimental

2.1. General

All manipulations were carried out under nitrogen atmosphere with standard Schlenk techniques. Reagent grade solvents were dried by the standard procedures and were freshly distilled prior to use. 2,7-Bis(diphenylphosphino)-1,8-naphthyridine (dpnapy) was prepared by the known method [5]. IR spectra were recorded on a JASCO FT/IR-410 spectrophotometer, and electronic absorption spectra were acquired on SHIMADZU UV-3100 and Hewlett–Packard Agilent 8453 spectrophotometers. ^1H and $^{31}P\{^1H\}$ NMR spectra were recorded on a Varian Gemini 2000 spectrometer at 300 and 121 MHz, respectively. ^1H NMR spectra were referenced to residual proto solvent or to TMS as external standard, and $^{31}P\{^1H\}$ NMR spectra were referenced to 85% H_3PO_4 as external standard. ESI-TOF mass spectra were recorded on an Applied Biosystems Mariner high-resolution mass spectrometer with positive ionization mode.

2.2. Synthesis of complexes

2.2.1. $[Rh_2(\mu\text{-dpnapy})_2(XylNC)_4](PF_6)_2$ (5)

Portions of $[RhCl(cod)]_2$ (51 mg, 0.10 mmol), XylNC (86 mg, 0.66 mmol), and NH_4PF_6 (99 mg, 0.61 mmol) were dissolved in CH_2Cl_2 (15 mL) and the mixture was stirred for 3 h at room temperature. To the resultant yellow suspension was added dpnapy (105 mg, 0.210 mmol). The color of the solution changed from yellow to dark red, which was further stirred over night at room temperature. After passing through a glass filter to remove inorganic salts, the solvent was removed under reduced pressure to dryness and the residue was washed with diethyl ether and extracted with a dichloromethane/methanol 1:1 mixed solvent (3 mL). Diethyl ether (ca. 3 mL) was carefully added to the solution, which was allowed to stand at 2 °C to afford orange microcrystals of $[Rh_2(\mu\text{-dpnapy})_2(XylNC)_4](PF_6)_2$ (**5**). Complex **5** was separated by filtration, washed with diethyl ether, and dried under vacuum (41 mg, yield 20%). Anal. Calc. for $C_{100}H_{84}N_8P_6F_{12}Rh_2$: C, 59.54; H, 4.20; N, 5.55. Found: C, 59.96; H, 4.30; N,

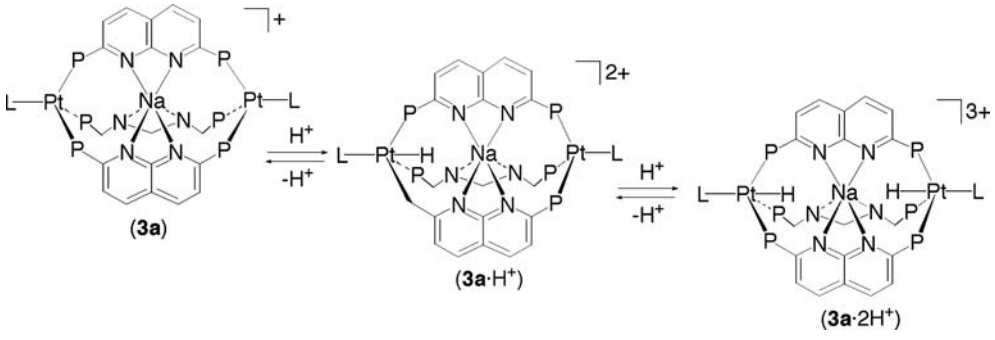

Scheme 2.

5.75%. IR (KBr, cm^{-1}): 2126 (N≡C), 840 (PF_6). UV–Vis (in CH_2Cl_2, nm (ε, $M^{-1}\,cm^{-1}$)): 411 (2.54×10^4), 322 (1.48×10^5). ^1H NMR (300 MHz, RT, CD_2Cl_2): δ 1.91 (s, 24H, *o*-Me), 6.7–8.1 (m, 60H, Ar). $^{31}P\{^1H\}$ NMR (121 MHz, RT, CD_2Cl_2): δ 32.9 (d, 4P, $^1J_{RhP}=121$ Hz). ESI-MS (in CH_2Cl_2): *m/z* 863.71 (*z*2, $\{Rh_2(dpnapy)_2(XylNC)_4\}^{2+}$ (863.70)).

2.2.2. $[Pt_2(\mu\text{-dpnapy})_2(XylNC)_4](PF_6)_4\cdot Et_2O$ (**6**$\cdot Et_2O$)

Portions of [$PtCl_2$(cod)] (78 mg, 0.21 mmol), XylNC (64 mg, 0.49 mmol), and NH_4PF_6 (204 mg, 1.25 mmol) were added in CH_2Cl_2 (15 mL) and the mixture was stirred for 5 h with warming at ca. 40 °C. To the resultant colorless suspension was added dpnapy (113 mg, 0.226 mmol). The color of the solution changed to pale yellow, and the mixture was stirred over night at room temperature. After passing through a glass filter to remove inorganic salts, the solvent was removed under reduced pressure to dryness and the residue was washed with diethyl ether and extracted with dichloromethane (3 mL). Diethyl ether (ca. 3 mL) was carefully added to the solution, and it was allowed to stand at 2 °C to afford pale pink powder of $[Pt_2(\mu\text{-dpnapy})_2(XylNC)_4](PF_6)_4\cdot Et_2O$ (**6**$\cdot Et_2O$) which was separated by filtration, washed with diethyl ether, and dried under vacuum (186 mg, yield 74%). Anal. Calc. for $C_{104}H_{94}N_8OP_8F_{24}Pt_2$: C, 48.68; H, 3.69; N, 4.37. Found: C, 48.70; H, 3.45; N, 4.33%. IR (KBr, cm^{-1}): 2209 (N≡C), 839 (PF_6). UV–Vis (in CH_2Cl_2, nm (ε, $M^{-1}\,cm^{-1}$)): 322 (3.29×10^4). ^1H NMR (300 MHz, RT, CD_2Cl_2): δ 1.15 (t, $(CH_3CH_2)_2O$), 1.94 (s, 24H, *o*-Me), 3.43 (q, $(CH_3CH_2)_2O$), 6.7–8.6 (m, 60H, Ar). $^{31}P\{^1H\}$ NMR (121 MHz, RT, CD_2Cl_2): δ 17.9 (s, 4P, $^1J_{PtP}=2069$ Hz). ESI-MS (in CH_2Cl_2): *m/z* 685.48 (*z*3, $\{Pt_2(dpnapy)_2(XylNC)_4(PF_6)\}^{3+}$ (685.49)), 1101.18 (*z*2, $\{Pt_2(dpnapy)_2(XylNC)_4(PF_6)_2H\}^{2+}$ (1101.22)).

2.2.3. $[Pd_2Cl_2(\mu\text{-dpnapy})_2(XylNC)_2](PF_6)_2\cdot 0.5CH_2Cl_2\cdot 0.5H_2O$ (**7**$\cdot 0.5CH_2Cl_2\cdot 0.5H_2O$)

[$PdCl_2$(cod)] (29 mg, 0.10 mmol), XylNC (54 mg, 0.41 mmol), and NH_4PF_6 (67 mg, 0.41 mmol) were mixed in CH_2Cl_2 (15 mL), which was stirred for 5 h with warming at ca. 40 °C. To the resultant pale yellow suspension was added dpnapy (55 mg, 0.11 mmol), and the mixture was stirred over night at room temperature. After passing through a glass filter to remove inorganic salts, the solvent was removed under reduced pressure to dryness and the residue was washed with diethyl ether and extracted with dichloromethane (2.5 mL). Addition of diethyl ether (ca. 4 mL) to the solution gave pale greenish yellow powder of $[Pd_2Cl_2(\mu\text{-dpnapy})_2(XylNC)_2](PF_6)_2\cdot 0.5CH_2Cl_2\cdot 0.5H_2O$ (**7**$\cdot 0.5CH_2Cl_2\cdot 0.5H_2O$) which were separated by filtration, washed with diethyl ether, and dried under vacuum (85 mg, yield 80%). The solvated water should be derived from wet sources of XylNC and NH_4PF_6. Anal. Calc. for $C_{82.5}H_{68}N_6O_{0.5}P_6F_{12}Cl_3Pd_2$: C, 52.58; H, 3.64; N, 4.46. Found: C, 52.35; H, 3.88; N, 4.78%. IR (KBr, cm^{-1}): 3630 br (H_2O), 2207 (N≡C), 839 (PF_6). UV–Vis (in CH_2Cl_2, nm (ε, $M^{-1}\,cm^{-1}$)): 359 (1.85×10^4), 330 (3.22×10^4). ^1H NMR (300 MHz, RT, CD_2Cl_2): δ 1.54 (s, H_2O), 1.87 (s, 12H, *o*-Me), 5.32 (s, CH_2Cl_2), 6.8–8.4 (m, 54H, Ar). ESI-MS (in CH_2Cl_2): *m/z* 771.11 (*z*2, $\{Pd_2Cl_2(dpnapy)_2(XylNC)_2\}^{2+}$ (771.09)).

2.2.4. $[Rh_2Ag(\mu\text{-dpnapy})_2(XylNC)_4](PF_6)_3\cdot 0.5CH_2Cl_2$ (**8**$\cdot 0.5CH_2Cl_2$)

A portion of $AgPF_6$ (7.2 mg, 0.028 mmol) was added to a dichloromethane solution (10 mL) of complex **5** (56 mg, 0.028 mmol). The solution was stirred for 2 days at room temperature in the dark, during which the color of the solution changed from pale orange to dark red. The solvent was removed under reduced pressure to dryness and the residue was washed with diethyl ether and extracted with dichloromethane (5 mL). The extract was concentrated to ca. 1 mL, to which vapor of diethyl ether (ca. 0.6 mL) was allowed to diffuse at room temperature. Dark red microcrystals of $[Rh_2Ag(\mu\text{-dpnapy})_2(XylNC)_4](PF_6)_3\cdot 0.5CH_2Cl_2$ (**8**$\cdot 0.5CH_2Cl_2$) were separated from the mother liquor, washed with diethyl ether, and dried under vacuum (22 mg, 34%). Anal. Calc. for $C_{100.5}H_{85}N_8P_7F_{18}ClAgRh_2$: C, 52.19; H, 3.70; N, 4.85. Found: C, 52.26; H, 3.96; N, 5.01%. IR (KBr, cm^{-1}): 2116 (N≡C), 840 (PF_6). UV–Vis (in CH_2Cl_2, nm (ε, $M^{-1}\,cm^{-1}$)): 435 (2.46×10^4), 326 (9.29×10^4). ^1H NMR (300 MHz, RT, CD_2Cl_2): δ 1.34 (s, 24H, *o*-Me), 5.32 (s, CH_2Cl_2), 6.8–8.6 (m, 60H, Ar), 7.94 (*d*, 4H, $^3J_{HH}=8.4$ Hz), 8.63 (*d*, 4H, $^3J_{HH}=8.4$ Hz). $^{31}P\{^1H\}$ NMR (121 MHz, RT, CD_2Cl_2): δ 35.2 (d, 4P, $^1J_{RhP}=130$ Hz). ESI-MS (in CH_2Cl_2): *m/z* 611.81 (*z*3, $\{Rh_2Ag(dpnapy)_2(XylNC)_4\}^{3+}$ (611.76)), 990.18 (*z*2, $\{Rh_2Ag(dpnapy)_2(XylNC)_4(PF_6)\}^{2+}$ (990.13)).

2.2.5. $\{[Rh(\mu\text{-dpnapy})(XylNC)_2](PF_6)\}_n\cdot nH_2O$ (**9**$\cdot nH_2O$)

An acetonitrile solution (15 mL) of complex **5** (43 mg, 0.022 mmol) was stirred over a droplet of mercury (~130 mg, 0.65 mmol) with ultrasonic vibration. Then, the solution was stirred for 2 days at room temperature. The solvent was removed to dryness and the residue was extracted with dichloromethane (5 mL). The extract was concentrated to ca. 1.5 mL, to which diethyl ether (ca. 0.7 mL) was added. The solution was allowed to stand at 2 ° C to afford yellow prismatic crystals of $\{[Rh(\mu\text{-dpnapy})(XylNC)_2](PF_6)\}_n\cdot nH_2O$ (**9**$\cdot nH_2O$), which were collected, washed with diethyl ether, and dried under vacuum (12 mg, 27%). Anal. Calc. for $C_{50}H_{44}N_4OP_3F_6Rh$: C, 58.49; H, 4.32; N, 5.46. Found: C, 58.49; H, 4.22; N, 5.47%. IR (KBr, cm^{-1}): 3660 br, 3590 br (H_2O), 2116 (N≡C), 839 (PF_6). UV–Vis (in CH_2Cl_2, nm (ε, $M^{-1}\,cm^{-1}$)): 411 (3.74×10^3), 322 (2.09×10^4). ESI-MS (in CH_2Cl_2): *m/z* 863.78 (*z*2, $\{Rh_2(dpnapy)_2(XylNC)_4\}^{2+}$ (863.70)), 1872.60 (*z*1, $\{Rh_2(dpnapy)_2(XylNC)_4(PF_6)\}^{+}$ (1872.35)).

2.3. X-ray crystallographic analyses of $8 \cdot 4.5CH_2Cl_2$ and $9 \cdot 1.25CH_2Cl_2 \cdot H_2O$

Crystal data and experimental conditions are summarized in Table 1. All data were collected at −120 °C on a Rigaku AFC8R/Mercury CCD diffractometer equipped with graphite-monochromated Mo Kα radiation using a rotating-anode X-ray generator. A total of 1440 oscillation images, covering whole sphere of $2\theta < 52°$, were collected with exposure rates of 256 (**8**) and 128 (**9**) s/° by ω scan method ($-70 < \omega < 110°$) with $\Delta\omega$ of 0.25 °. The crystal-to-detector (70×70 mm) distance was set to 60 mm. The data were processed using Crystal Clear 1.3.5 program (Rigaku/MSC) [10] and corrected for Lorentz-polarization and absorption effects. The structure of $\mathbf{8} \cdot 4.5CH_2Cl_2$ was solved by heavy atom methods (DIRDIF 94 Patty) [11], and refined on F with full-matrix least squares techniques with TEXSAN [12]. The Ag, Rh, Cl, P, and F atoms were refined with anisotropic thermal parameters, and the N and C atoms were refined isotropically. The positions of hydrogen atoms were calculated and fixed in the refinement. The Ag atom was disordered in two sites, Ag1 and Ag2, with 2:1 population. The PF_6 anion with the P14 atom was treated as a rigid group with 0.5 occupancy. The structure of $\mathbf{9} \cdot 1.25CH_2Cl_2 \cdot H_2O$ was solved by heavy atom methods (DIRDIF 94 Patty) [11], and refined on F^2 by least squares techniques with SHELXL-93 [13]. All the non-hydrogen atoms, other than the O and C atoms of solvent molecules, were refined anisotropically. All C–H hydrogen atoms except those of solvent molecules were calculated and fixed in the refinement. The solvent molecules of crystallization were determined as $1.25CH_2Cl_2$ and H_2O with disordered structures. All calculations were carried out on a Silicon Graphics O2 station with TEXSAN crystallographic software package and a Pentium PC with Crystal Structure package [14].

Table 1
Crystallographic and experimental data for compounds $\mathbf{8} \cdot 4.5CH_2Cl_2$ and $\mathbf{9} \cdot 1.25CH_2Cl_2 \cdot H_2O$

Compound	$\mathbf{8} \cdot 4.5CH_2Cl_2$	$\mathbf{9} \cdot 1.25CH_2Cl_2 \cdot H_2O$
Formula	$C_{104.5}H_{93}N_8P_7F_{18}Cl_9Rh_2Ag$	$C_{51.25}H_{46.5}N_4P_3F_6Cl_{2.5}ORh$
Fw	2652.48	1132.91
Crystal system	Triclinic	Trigonal
Space group	$P\bar{1}$ (*no.* 2)	$P3_112$ (no. 151)
a (Å)	15.580(2)	17.8750(5)
b (Å)	18.173(2)	
c (Å)	24.429(3)	33.514(1)
α (°)	102.710(3)	
β (°)	104.655(3)	
γ (°)	107.737(3)	
V (Å^3)	6033(1)	9273.6(5)
Z	2	6
T (°C)	−120	−120
D_{calc} (g cm^{-3})	1.460	1.217
Abs. coeff. (cm^{-1})	7.96	5.14
2θ Range (°)	$6 < 2\theta < 52$	$6 < 2\theta < 52$
No. of unique data	14265	4718
No. of obsd. data	9342 ($I > 3\sigma(I)$)	3273 ($I > 2\sigma(I)$)
No. of variables	808	666
R[a]	0.134	0.107
R_w[b] or wR_2[c]	0.143[b]	0.328[c]

[a] $R = \sum\|F_o| - |F_c\|/\sum|F_o|$.
[b] $R_w = [\sum w(|F_o| - |F_c|)^2/\sum w|F_o|^2]^{1/2} (w = 1/\sigma^2(F_o))$.
[c] $wR_2 = [\sum w(F_o^2 - F_c^2)^2/\sum w(F_o^2)^2]^{1/2}$ (for all data).

2.4. Molecular orbital calculations

Single point density functional calculations on the structures of **8** (determined by X-ray crystallography) and the hypothetical intermediate structure **I** (Scheme 4) were performed using the BECK3LYP method with the LANL2DZ basis set. All calculations were carried out on a Silicon Graphic Octane Station with the GAUSSIAN 98 program package.

3. Results and discussion

3.1. Syntheses of d^8 dinuclear complexes with dpnapy, $[M_2(\mu\text{-dpnapy})_2(XylNC)_4](PF_6)_n$ (5: M = Rh, n = 2; 6: M = Pt, n = 4)

When $[RhCl(cod)]_2$ was treated with dpnapy in the presence of XylNC and NH_4PF_6 in CH_2Cl_2, orange microcrystals of $[Rh_2(\mu\text{-dpnapy})_2(XylNC)_4](PF_6)_2$ (**5**) were isolated in a yield of 20% (Scheme 3). A similar procedure using $[PtCl_2(cod)]$ produced $[Pt_2(\mu\text{-dpnapy})_2(XylNC)_4](PF_6)_4$ (**6**) in good yields (Scheme 3). The IR spectra of **5** and **6** showed a peak for N≡C stretching bands at 2126 and 2209 cm^{-1}, respectively, suggesting the presence of terminal isocyanides in a mutual *trans*–arrangement with respect to the square planar metal center. In the ^{1}H NMR spectra, a singlet resonance for *o*-methyl protons of XylNC was observed at δ 1.91 ppm (**5**) and 1.94 ppm (**6**). The peak intensities for the methyl and aromatic protons suggested that the ratio of XylNC and dpnapy is 2:1. The $^{31}P\{^1H\}$ NMR spectrum of complex **5** exhibited a doublet peak for the dpnapy ligand at δ 32.9 ppm with $^1J_{RhP} = 121$ Hz, and the same peak appeared as a singlet at δ 17.9 ppm for **6** with ^{195}Pt satellite peaks ($^1J_{PtP} = 2069$ Hz). The ESI mass spectrum of **5** showed an intense divalent peak at m/z 863.71 corresponding to $\{Rh_2(dpnapy)_2(XylNC)_4\}^{2+}$ and that of **6** showed trivalent and divalent cation peaks at m/z 685.48 and 1101.18 assignable to $\{Pt_2(dpnapy)_2(XylNC)_4(PF_6)\}^{3+}$ and $\{Pt_2(dpnapy)_2(XylNC)_4(PF_6)_2\}^{2+}$,

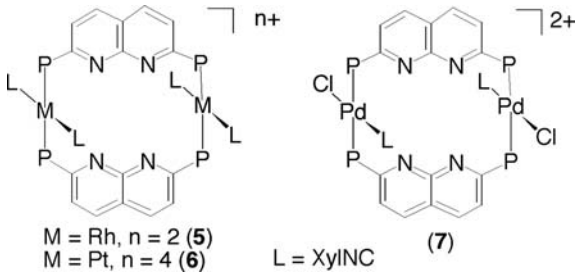

Scheme 3.

respectively. These spectral features of **5** and **6** are suggestive of the metallomacrocyclic structures as shown in Scheme 3. By a procedure similar to that for **6**, $[PdCl_2(cod)]$ was converted into the dinuclear Pd(II) complex formulated as $[Pd_2Cl_2(\mu\text{-dpnapy})_2(XylNC)_2](PF_6)_2$ (**7**), which was characterized by elemental analysis and spectroscopic techniques.

3.2. Incorporation of Ag(I) ion by complex 5 affording $[Rh_2Ag(\mu\text{-dpnapy})_2(XylNC)_4](PF_6)_3$ (8)

The dinuclear Rh(I) macrocycle of **5** readily reacted with $AgPF_6$ to yield dark red microcrystals of $[Rh_2Ag(\mu\text{-dpnapy})_2(XylNC)_4](PF_6)_3$ (**8**) in an isolated yield of 34% (Scheme 4). The NMR spectra of **8** at room temperature in CD_2Cl_2 exhibited a symmetrical structure for the $\{Rh_2(\mu\text{-dpnapy})_2(XylNC)_4\}$ framework; in the ^1H NMR spectrum, a singlet peak for *o*-methyl protons of XylNC was shifted to δ 1.34 from δ 1.91 ppm (**5**), and in the $^{31}P\{^1H\}$ NMR spectrum, a doublet peak for the dpnapy ligand appeared at δ 35.2 ppm with $^1J_{RhP} = 130$ Hz (Fig. 1). The ESI mass spectrum in CH_2Cl_2 exhibited intense di- and trivalent peaks at $m/z = 990.18$ and 611.81 corresponding to $\{Rh_2Ag(dpnapy)_2(XylNC)_4(PF_6)\}^{2+}$ and $\{Rh_2Ag(dpnapy)_2(XylNC)_4\}^{3+}$, respectively, and indicated that a silver(I) ion is trapped in the $\{L_2Rh(\mu\text{-dpnapy})_2RhL_2\}^{2+}$ (L = XylNC) metallomacrocycle in the solution state (Fig. 2). The Ag(I) incorporation was monitored by UV–Vis spectral titration as shown in Fig. 3. From the increments of the band at 435 nm, the binding constant was estimated as 8.3×10^3.

The detailed structure of complex **8** was determined by X-ray crystallography; ORTEP plot for the complex cation is illustrated in Fig. 4 and selected bond distances and angles are summarized in Table 2. The complex cation of **8** is comprised of two rhodium(I) ions bridged by two dpnapy ligands to form a $\{Rh_2(\mu\text{-dpnapy})_2\}$ framework, which is further coordinated by two terminal isocyanide ligands for each metal center (Fig. 4a). Each Rh(I) center has a *trans*-$[P_2C_2]$ square planar geometry comprised of two P atoms of dpnapy ligands and two isocyanide C atoms (av. Rh–P = 2.310 Å, av. Rh–C = 1.90 Å). The two square planes are nearly parallel in ca. 90°–twisted eclipsed form (Fig. 4b). The Rh1···Rh2 distance is 7.438(2) Å, which is significantly shorter than that of the diplatinum(0) complex

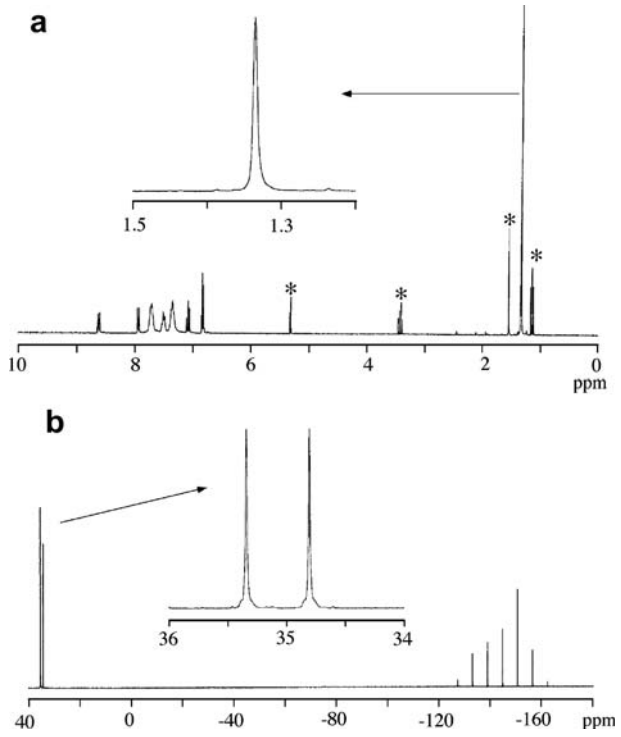

Fig. 1. (a) ^1H and (b) $^{31}P\{^1H\}$ NMR spectra of $[Rh_2Ag(\mu\text{-dpnapy})_2(XylNC)_4](PF_6)_3$ (**8**) in CD_2Cl_2 at room temperature. Peaks with asterisk were derived from impurity.

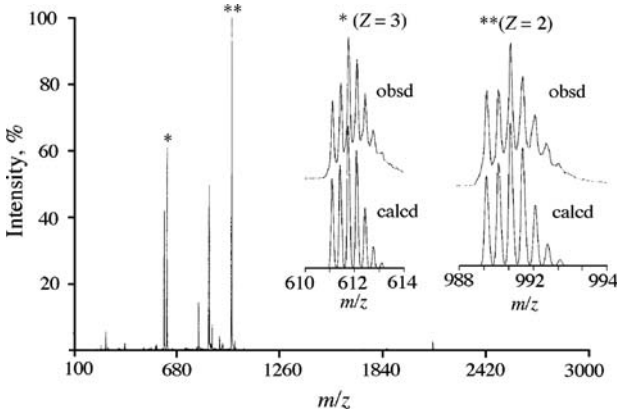

Fig. 2. ESI mass spectrum for a dichloromethane solution of $[Rh_2Ag(\mu\text{-dpnapy})_2(XylNC)_4](PF_6)_3$ (**8**) at room temperature. The inset views indicate the observed and calculated spectral patterns for di- and trivalent peaks around $m/z = 990.18$ and 611.81 corresponding to $\{Rh_2Ag(dpnapy)_2(XylNC)_4(PF_6)\}^{2+}$ and $\{Rh_2Ag(dpnapy)_2(XylNC)_4\}^{3+}$, respectively.

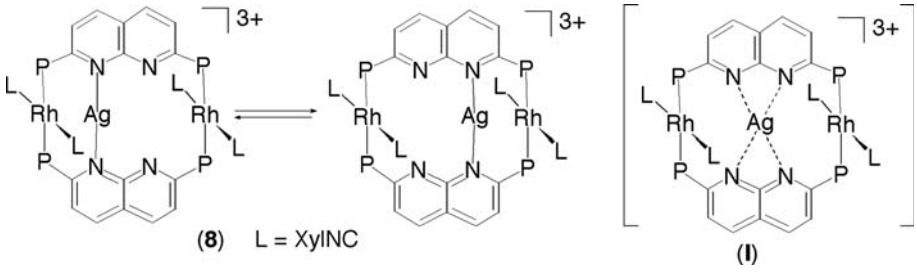

Scheme 4.

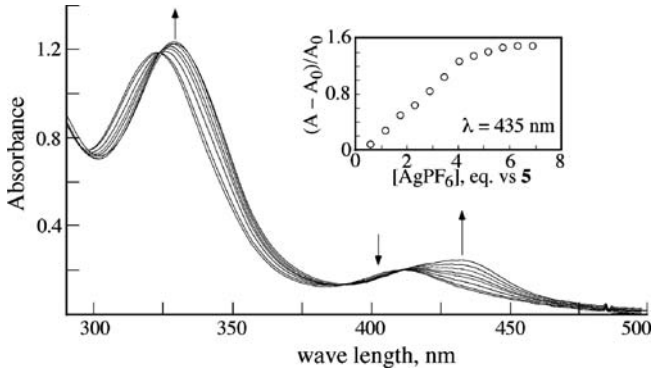

Fig. 3. Electronic absorption spectral changes for titration of **5** with $AgPF_6$ in dichloromethane at room temperature.

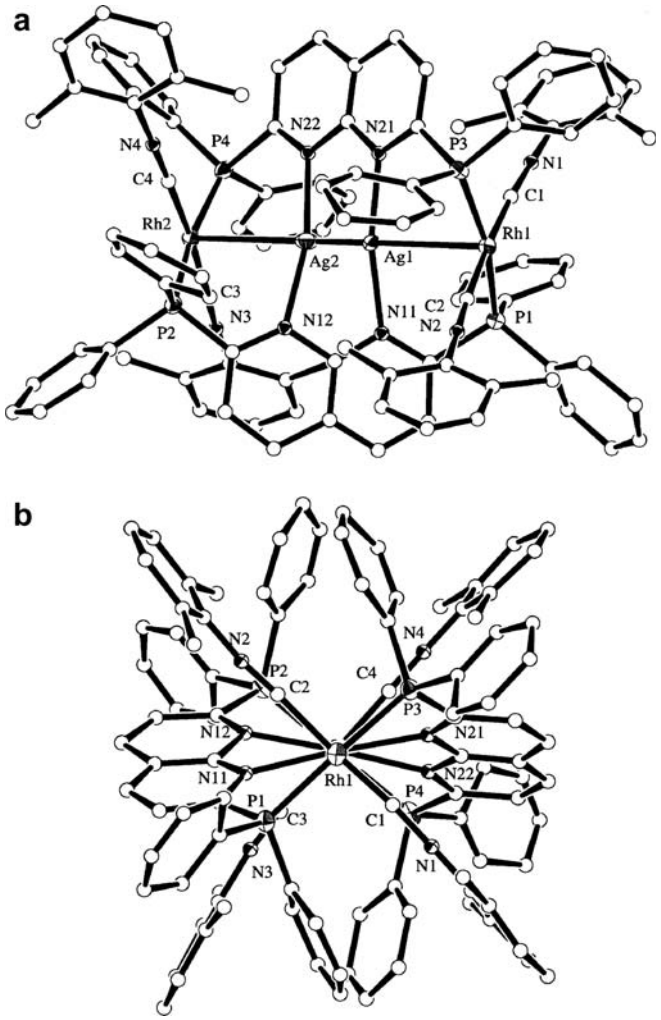

Fig. 4. (a) ORTEP plot for the complex cation of **8**, $[Rh_2Ag(\mu\text{-dpnapy})_2(XylNC)_4]^{3+}$. The carbon and nitrogen atoms are drawn with ideal circles for clarity. (b) ORTEP view for the complex cation of **8**, viewed along the Rh–Ag–Rh axis.

with three dpnapy ligands (**3a**, Pt···Pt = 8.4601(7) Å) and is longer than that found in the dinuclear Au(I) complex **2a** (Au···Au = 7.126(2) Å). In the {Rh(PNNP)$_2$Rh} macrocycle, a silver(I) ion is incorporated, but is disordered in the two positions determined as Ag1 and Ag2 with a population of 2:1. The separation between two disordered sites of the Ag ion is 1.606(5) Å (Ag1···Ag2). Each Ag atom is linearly ligated by the two N atoms of dpnapy ligands (av. Ag–N = 2.20 Å, av. N–Ag–N = 166.7 °). The Ag positions are slightly deformed toward the center of the macrocycle from the linear N–Ag–N ideal positions. The shorter Rh···Ag interatomic distances are 2.908(3) Å (Ag1–Rh1) and 2.926(5) Å (Ag2–Rh2), indicating the absence of Ag–Rh bonding interaction. The Ag–Rh vectors are almost perpendicular to the Rh(I) coordination planes.

3.3. Site-exchange behavior of the Ag(I) ion incorporated into the {$Rh_2(\mu$-dpnapy$)_2$(XylNC$)_4$} macrocycle

While the X-ray crystal structure revealed the disordered Rh–Ag···Rh asymmetric structure, the ^{1}H and ^{31}P{^{1}H} NMR spectra of **8** at room temperature are consistent of a C_2 symmetrical structure as mentioned above, which demonstrated a rapid site-exchange behavior of the trapped Ag(I) ion as indicated in Scheme 4. Whereas some attempts with low temperature NMR studies were performed to determine the exchange rate, the ^{31}P{^{1}H} and ^{1}H NMR spectra for **8** were invariant at −80 °C in CD_2Cl_2, indicating that the dynamic behavior is faster than the NMR time scale even at low temperature.

To understand the electronic structure, single–point DFT molecular orbital calculations were carried out on the X-ray determined structure of **8**. Some important MO diagrams are illustrated in Fig. 5. The HOMO is a non-bonding orbital (n_d) composed of the out-of-plane $d\sigma$ orbital on the Rh atom far from the Ag ion. The LUMO and LUMO + 1 orbitals are predominantly made of π^* orbitals of the naphthyridine units. The σ_d and σ_d^* interactions between the Ag and the Rh atoms (2.908 Å apart) are observed in the low-laying HOMO − 34 and HOMO − 3 orbitals, respectively, both being occupied and suggesting the absence of bonding interaction between them. DFT calculations were also performed on the postulated symmetrical intermediate structure (**I** in Scheme 4) to provide a total energy higher only by ca. 5.0 kJ/mol than that for **8**. These results implied that the activation energy for the site-exchange pathway of Ag(I) ion could be very small owing to the absence of significant Ag–Rh bonding interaction. Furthermore from these results, it should be noted that the possibility of the Rh···Ag···Rh symmetrical structure (**I**) in the solution state could not thoroughly be ruled out.

3.4. Transformation of 5 into C_6 helical polymer of {[Rh(μ-dpnapy)(XylNC)$_2$](PF$_6$)}$_n$ (9)

When complex **5** is treated in acetonitrile over a drop of mercury, the dirhodium(I) complex **5** was converted into the yellow polymeric compounds formulated as {[Rh(μ-dpnapy)(XylNC)$_2$](PF$_6$)}$_n$ (**9**) (Scheme 5). The structure of

Table 2
Selected bond lengths (Å) and angles (°) for $[Rh_2Ag(\mu\text{-dpnapy})_2(XylNC)_4](PF_6)_3$ (**8**)

Rh1–P1	2.312(4)	Rh2–P2	2.309(5)
Rh1–P3	2.308(4)	Rh2–P4	2.312(6)
Rh1–C1	1.79(2)	Rh2–C3	1.92(1)
Rh1–C2	1.99(2)	Rh2–C4	1.90(1)
C1–N1	1.35(3)	C3–N3	1.14(2)
C2–N2	1.17(3)	C4–N4	1.24(2)
Ag1–N11	2.21(1)	Ag2–N12	2.19(1)
Ag1–N21	2.17(1)	Ag2–N22	2.24(1)
Rh1···Ag1	2.908(3)	Rh2···Ag2	2.926(5)
Ag1–Rh1–P1	84.3(1)	Ag2–Rh2–P2	83.8(2)
Ag1–Rh1–P3	82.9(1)	Ag2–Rh2–P4	86.2(2)
Ag1–Rh1–C1	92.7(6)	Ag2–Rh2–C3	91.6(6)
Ag1–Rh1–C2	92.2(6)	Ag2–Rh2–C4	92.5(5)
P1–Rh1–P3	167.1(2)	P2–Rh2–P4	169.9(2)
P1–Rh1–C1	93.5(5)	P2–Rh2–C3	89.0(6)
P1–Rh1–C2	90.0(4)	P2–Rh2–C4	90.3(5)
P3–Rh1–C1	85.0(5)	P4–Rh2–C3	92.4(6)
P3–Rh1–C2	92.6(4)	P4–Rh2–C4	89.0(5)
C1–Rh1–C2	174.2(7)	C3–Rh2–C4	175.7(7)
N11–Ag1–N21	168.2(5)	N12–Ag2–N22	165.1(6)
Rh1–C1–N1	175(1)	Rh2–C3–N3	172(1)
Rh1–C2–N2	176(1)	Rh2–C4–N4	178(1)
C1–N1–C11	179(1)	C3–N3–C31	172(1)
C2–N2–C21	172(1)	C4–N4–C41	178(1)

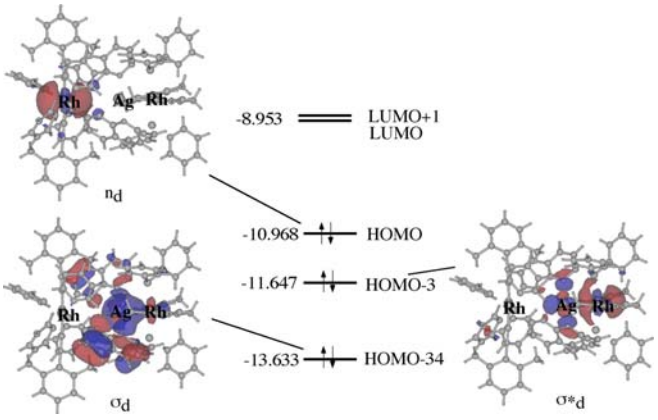

Fig. 5. MO diagrams for $[Rh_2Ag(\mu\text{-dpnapy})_2(XylNC)_4]^{3+}$ on the basis of DFT single-point calculations.

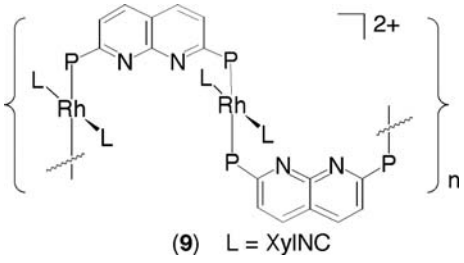

Scheme 5.

9 was determined by X-ray crystallography; ORTEP plots for the units of the complex cation are shown in Fig. 6a and b and some selected bond distances and angles are listed

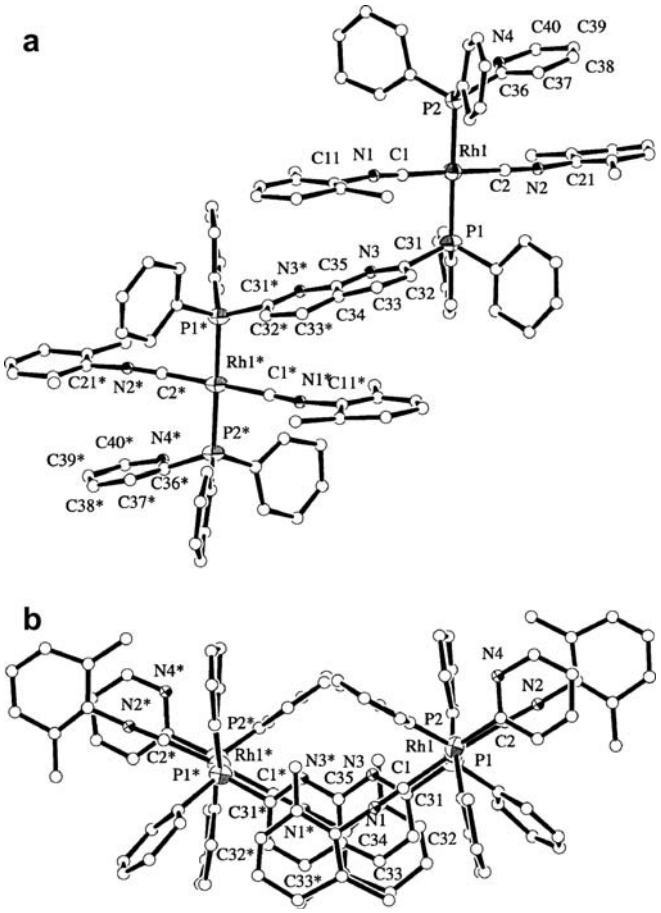

Fig. 6. (a) ORTEP plot for the complex cation chain of **9**, $\{[Rh(\mu\text{-dpnapy})(XylNC)_2]^+\}_n$. The carbon and nitrogen atoms are drawn with ideal circles for clarity. (b) ORTEP view for the complex cation chain of **9**, viewed vertical to the naphthyridine plane.

Table 3
Selected bond lengths (Å) and angles (°) for $\{[Rh(\mu\text{-dpnapy})(XylNC)_2](PF_6)\}_n$ (**9**)

Rh1–P1	2.292(1)	Rh1–P2	2.308(1)
Rh1–C1	1.938(5)	Rh1–C2	1.925(5)
C1–N1	1.093(7)	C2–N2	1.182(6)
P1–Rh1–P2	178.16(6)	P1–Rh1–C1	89.3(2)
P1–Rh1–C2	89.4(1)	C1–Rh1–C2	176.2(3)
P2–Rh1–C2	90.9(1)	P2–Rh2–C1	90.3(2)
Rh1–P1–C31	111.9(2)	Rh1–P2–C36	115.3(2)
Rh1–C1–N1	178.0(5)	Rh1–C2–N2	176.6(5)
C1–N1–C11	171.4(6)	C2–N2–C21	173.5(5)

in Table 3. The *trans*-$\{Rh(I)(XylNC)_2\}^+$ mononuclear units are connected by the phosphine units of dpnapy ligands, resulting in the polymeric chain of $\{[Rh(\mu\text{-dpnapy})(XylNC)_2]^+\}_n$ (Fig. 6a). With respect to the naphthyridine plane, the two Rh(I) atoms are in *anti*–arrangement, leading to the C_6 helical structure along *c* axis with a pitch of 33.5 Å (rise of unit = 5.6 Å) and a diameter of 20.64 Å (Fig. 7a and b). Although a role of mercury atom is not clear at all, it might partake in the ring–opening–process of $\{Rh(PNNP)_2Rh\}^{2+}$ in **5**. Compound **9**, dissolved in

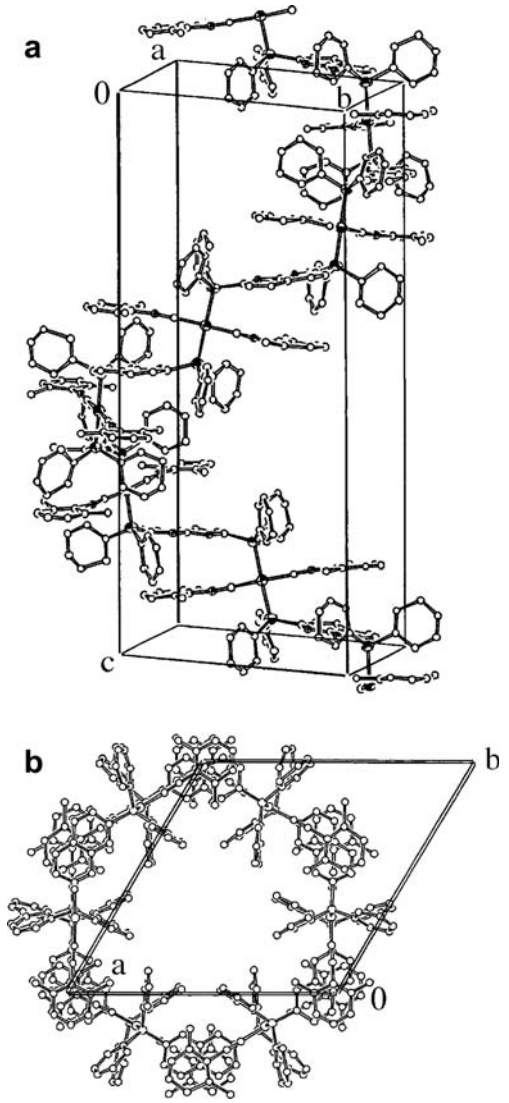

Fig. 7. (a) Packing diagram for the complex cation chain of **9**, $\{[Rh(\mu\text{-dpnapy})(XylNC)_2]^+\}_n$. (b) Packing diagram for the complex cation chain of **9**, viewed along *c* axis.

dichloromethane, partially regenerated the dirhodium(I) complex **5**, which was confirmed by ESI mass spectroscopy.

4. Conclusion

In the present study, dinuclear complexes containing a small and rigid d^8 $\{M_2(\mu\text{-dpnapy})_2\}$ metallomacrocycle, $[Rh_2(\mu\text{-dpnapy})_2(XylNC)_4](PF_6)_2$ (**5**), $[Pt_2(\mu\text{-dpnapy})_2(XylNC)_4](PF_6)_4$ (**6**), and $[Pd_2Cl_2(\mu\text{-dpnapy})_2(XylNC)_2](PF_6)_2$ (**7**), were synthesized using the rigid PNNP ligand, 2,7-bis(diphenylphosphino)-1,8-naphthyridine (dpnapy). Complex **5** readily incorporated a silver(I) ion into the macrocycle to produce $[Rh_2Ag(\mu\text{-dpnapy})_2(XylNC)_2](PF_6)_3$ (**8**), in which a Ag(I) ion is trapped by two *trans* N atoms of dpnapy ligands, resulting in an asymmetric Rh–Ag···Rh structure, in the crystal structure, and however, in a CH_2Cl_2 solution, a dynamic exchange of the Ag–trapped sites was observed. Complex **5**, treated with mercury in acetonitrile, was transformed to the polymeric compound of $\{[Rh(dpnapy)(XylNC)_2](PF_6)\}_n$ (**9**), which were revealed to consist of the C_6helical structure along *c* axis. These results suggested that the d^8 metallomacrocyale, $\{M(dpnapy)_2M\}$ could be a useful building block toward heterometallic functional systems with dynamic properties.

5. Supplementary material

Crystallographic data for the structural analysis have been deposited with Cambridge Crystallographic Data Center, CCDC Nos. 600792 and 600793 for complexes **8** and **9**, respectively. Copies of this information may be obtained free of charge from The Cambridge Crystallographic Data Center, 12 Union Road, Cambridge, CB21EZ, UK (Fax: +44 1223 336033; e-mail: deposit@ccdc.cam.ac.uk or www: http://www.ccd.cam.ac.uk).

Acknowledgement

This work was partly supported by Grant-in-Aid for Scientific Research on Priority Areas (Reaction Control of Dynamic Complexes) from Ministry of Education, Culture, Sports, Science, and Technology of Japan.

References

[1] (a) D.A. Adams, F.A. Cotton (Eds.), Ctalysis by Di- and Polynuclear Metal Cluster Complexes, Wiley-VCH, New York, 1998;
(b) A.L. Balch, in: L.H. Pignolet (Ed.), Homogeneous Catalysis with Metal Phosphine Complexes, Plenum Press, New York, 1983, p. 167;
(c) J.H. Sinfelt, Bimetallic Catalysis: Discoveries, Concepts and Applications, Wiley, New York, 1983;
(d) L. Guczi, in: G.C. Gates, L. Guczi, H. Knozinger (Eds.), Metal Clusters in Catalysis, Elsevier, New York, 1986;
(e) L.J. Farrygia, Adv. Organomet. Chem. 31 (1990) 301;
(f) P. Braunstein, J. Rose, in: R.D. Adams (Ed.), Comprehensive Organometallic Chemistry II, vol. 10, Elsevier, New York, 1995, p. 351.
[2] V.J. Catalano, B.L. Bennett, M.A. Malwitz, R.L. Yson, H.M. Kar, S. Muratidis, S.J. Horner, Comments Inorg. Chem. 24 (2004) 39.
[3] (a) V.J. Catalano, B.L. Bennett, H.M. Kar, J. Am. Chem. Soc. 121 (1999) 10235;
(b) V.J. Catalano, B.L. Bennett, B.C. Noll, Chem. Commun. (2000) 1413;
(c) V.J. Catalano, B.L. Bennett, R.L. Yson, B.C. Noll, J. Am. Chem. Soc. 122 (2000) 10056;
(d) V.J. Catalano, M.A. Malwitz, B.C. Noll, Chem. Commun. (2001) 581;
(e) V.J. Catalano, M.A. Malwitz, B.C. Noll, Inorg. Chem. 41 (2002) 6553.
[4] (a) V.J. Catalano, H.M. Kar, J. Garnas, Angew. Chem., Int. Ed. 38 (1999) 1979;
(b) V.J. Catalano, M.A. Malwitz, S.J. Horner, J. Vasquez, Inorg. Chem. 42 (2003) 2141;
(c) S.-M. Kuang, L.-M. Zhang, Z.-Z. Zhang, B.-M. Wu, T.C.W. Mak, Inorg. Chim. Acta 284 (1999) 278.
[5] R. Ziessel, Tetrahedron Lett. 30 (1989) 463.
[6] R.-H. Uang, C.-K. Chan, S.-M. Peng, C.-M. Che, J. Chem. Soc., Chem. Commun. (1994) 2561.
[7] V.J. Catalano, H.M. Kar, B.L. Bennett, Inorg. Chem. 39 (2000) 121.

[8] E. Goto, M. Usuki, H. Takenaka, K. Sakai, T. Tanase, Organometallics 23 (2004) 6042.
[9] T. Tanase, T. Igoshi, K. Kobayashi, Y. Yamamoto, J. Chem. Res. (S) (1998) 538.
[10] CRYSTAL CLEAR 1.3.5: Operating software for the CCD detector system. Rigaku and Molecular Structure Corp., 2003.
[11] P.T. Beurskens, G. Admiraal, G. Beurskens, W.P. Bosman, R. de Gelder, R. Israel, J.M.M. Smits, DIRDIFF-94 program system, Technical Report of the Crystallography Laboratory, University of Nijmegen, The Netherlands, 1994.
[12] TEXSAN: Crystal Structure Analysis Package, Molecular Structure Corp., 1999.
[13] G.M. Sheldrick, SHELXL-97: Program for the Refinement of Crystal Structures, University of Göettingen, Göettingen, Germany, 1996.
[14] CRYSTAL STRUCTURE 3.6: Crystal Structure Analysis Package, Rigaku and Molecular Structure Corp., 2003.